Solar RRL

WILEY VCH

Solar RRL

RESEARCH ARTICLE OPEN ACCESS

Improved ZnO Post-Treatment for High Performance Organic Solar Cell Materials

Jonas Wortmann[1,2] | Xiaoyan Du[3] | Jerrit Wagner[2] | Paul Weitz[1] | Simon Arnold[2] | Chao Liu[1,2] | Vincent M. Le Corre[1] | Anastasiia Barabash[1,2] | Jens Hauch[2] | Thomas Heumüller[1,2] | Christoph J. Brabec[1,2]

[1]Department of Materials Science and Engineering, Institute of Materials for Electronics and Energy Technology (i-MEET), Friedrich-Alexander-Universität Erlangen-Nürnberg, Erlangen, Germany | [2]Department of High Throughput Methods in Photovoltaics, Helmholtz Institute Erlangen-Nürnberg for Renewable Energy (HI ERN), Forschungszentrum Jülich GmbH, Erlangen, Germany | [3]School of Physics, Shandong University, Jinan, P. R.China

Correspondence: Jonas Wortmann (j.wortmann@fz-juelich.de) | Thomas Heumüller (thomas.heumueller@fau.de) | Christoph J. Brabec (christoph.brabec@fau.de)

Received: 13 March 2025 | **Revised:** 12 June 2025 | **Accepted:** 20 June 2025

Funding: Helmholtz Association;; European Union's Horizon 2020 research and innovation program, Grant/Award Numbers: 952911, 101137889 952911, 101137889; Deutsche Forschungsgemeinschaft, Grant/Award Number: 461909888; ELF-PV, Grant/Award Number: 44-6521a/20/4; Aufbruch Bayern; Solar Technologies go Hybrid

Keywords: light soaking | low temperature processing | organic solar | PM6:Y6 | zink oxide

ABSTRACT

Zinc oxide (ZnO) is a widely used electron transport layer for organic solar cells which has been optimized and established for the first generation of organic photovoltaic (OPV) materials. With the emergence of novel OPV materials which can reach up to 20% efficiency, several limitations of ZnO have become apparent. In particular, interactions of the active layer with ZnO under illumination can severely limit the device efficiency and stability. In this study, we investigate how various treatment options of ZnO like thermal annealing, ultraviolet exposure, as well as vacuum treatment can improve ZnO properties. Calcium tests show the release of reactive components form ZnO, and space charge limited current measurements allow to model energy level alignment using drift diffusion simulations. Crucially, permanent J_{sc} losses related to insufficient treatment of ZnO are observed for high performing material systems. An additional UV treatment step under vacuum is shown to significantly reduce those J_{sc} losses and allows using ZnO annealing temperatures of only 80°C.

1 | Introduction

In recent years, organic solar cells (OSCs) have made tremendous improvements in efficiencies, reaching around 20% [1]. One of the reasons for the big improvements is the development of novel active layer materials, especially nonfullerene acceptors (NFA) [2].

Inorganic n-type zinc oxide (ZnO), which possesses high transmittance and conductivity, as well as electron charge selectivity, is a commonly used electron transporting material (ETM) in OSCs [3–5]. Furthermore, ZnO can be processed at low temperatures for roll-to-roll processing on flexible polymer substrates [6, 7], and advanced structural control is possible with nanofibers [8]. Under ultraviolet (UV) illumination, ZnO can show a sudden increase of conductivity which has been named the "light-soaking" effect and was first described in the 1950s [9, 10]. Previous studies describe a mechanism where UV light can release oxygen from a ZnO film in gaseous form, leaving valence electrons in the vacant site and thus increasing conductivity [11, 12]. Using mass spectrometry, oxygen and water have been observed to desorb from ZnO under UV illumination [13]. Impedance analysis of ZnO layers allows distinguishing the effect of water and oxygen on ZnO conductivity, which can be seen in a low frequency and high frequency component, respectively [13]. Upon exposure to wet nitrogen, a strong low

frequency component attributed to water is visible, which disappears upon immersion in pure nitrogen indicating that water is physiosorbed and can be removed effectively. In contrast to this, the high frequency component of the impedance spectrum only disappears after UV illumination under nitrogen and is attributed to the chemisorption of oxygen on ZnO [13]. Moreover, also CO_2 release from ZnO layers has been detected in mass spectrometry suggesting that in the presence of UV light, photocatalytic reaction of ZnO with hydrocarbons may occur [14].

The light-soaking issues of ZnO have been reported for various deposition methods (sol–gel [15], spray coating [16], NP deposition [17]). In the literature, lots of research is ongoing towards replacing ZnO, e.g. with AZO [15, 18, 19], with SnO_2 [20, 21] and more recently with TiO_x [22, 23, 24]. Nevertheless at the moment, ZnO remains the state of the art interface layer for roll-to-roll processing in ambient atmosphere and a certain amount of oxygen inside the ZnO layer seems inevitable leading to light soaking effects and re-distribution of oxygen inside the device upon illumination [25].

Most of the investigations on light soaking in the presence of ZnO were performed on first generation organic photovoltaic (OPV) materials including P3HT:PCBM where the adverse effects of ZnO could be managed by UV-light soaking [25]. Moreover, solution processed ZnO nanoparticles were optimized to provide good device performance in P3HT:PCBM at annealing temperatures as low as 80°C. Early tests of novel material systems, in particular PM6:Y6, showed surprisingly low device performance of only 4% efficiency when annealing ZnO at 80°C. By increasing the annealing temperature to 150°C, the performance increased to 12%, and annealing of ZnO at 250°C resulted in the best device performance [26]. Studies on photo-oxidation of a series of novel non-fullerene acceptors (NFA) show up to two orders of magnitude faster photo-oxidation for some NFA materials like ITIC when compared to PCBM or IDTBR [27]. This increased sensitivity of ITIC (and also Y6) to oxygen in photo-oxidation tests could cause detrimental effects in solar cells, when oxygen is released from a ZnO layer. So while a reduction of oxygen in the ZnO layer is desirable from a stability perspective, UV pretreatment of ZnO to remove oxygen can reduce conductivity [13] and has been linked to lower starting efficiency [28].

In this study, we investigate different post-treatment options for ZnO layers to manage the content of adsorbed oxygen and its effects on initial device performance as well as device stability. In particular, we will compare different donor and acceptor materials and focus on the interactions between interlayer and active layer. Furthermore, we investigate different methods to directly (and indirectly) identify interface effects related to ZnO and SnO_2 interface layers. While SnO_2 reduces light soaking effects, significant limitations in photostability of solar cells have been observed when using this interlayer material [29]. A range of different treatment conditions for ZnO is applied including thermal annealing at different temperatures as well as illumination with UV light in nitrogen or vacuum. In a first test, metallic calcium is evaporated on top of the treated ZnO layers which will form transparent reaction products in the presence of oxygen or water. To indirectly probe changes of energy level alignment between ZnO and organic active layers, space charge limited current (SCLC) measurements are performed on electron only devices. Modeling the current voltage characteristics of those devices with drift diffusion simulations allows detailed insight into energetic injection or extraction barriers. Moreover, electroluminescence (EL) images are used to perform noninvasive in situ investigations and to detect spatial inhomogeneity. A range of different donor and acceptor materials in full soar cells is used to investigate the relative sensitivity of different active layer materials to the effects of ZnO.

2 | Results and Discussion

In the first experiments, we investigate the effect of different treatments on ZnO and SnO_2 layers. Figure 1a shows SEM images for ZnO layers spincoated on indium tin oxide (ITO) glass and annealed at 80°C with and without UV light treatment as well as annealing at 200°C. The SEM images show no significant change of the ZnO layer upon annealing or UV light treatment. In a second experiment, a thin layer (40 nm) of metallic calcium was evaporated on top of ZnO layers which had previously undergone different treatment conditions using the same mask and evaporator as for solar cell production. The high reactivity of metallic calcium with oxygen (and water) results in the fast formation of transparent reaction products, which can be seen readily. In Figure 1b, strong differences can be observed for the ZnO annealed at 80°C and 200°C. At 80°C, almost complete oxidation of calcium is observed, whereas at 200°C, partial preservation of elemental calcium is possible. When the 200°C annealing treatment is followed by UV exposure under nitrogen, the extent of oxidation is further reduced. The highest quality ZnO layer is obtained by a UV treatment in vacuum using a glovebox antechamber and a battery powered UV light-emitting diode (LED) (Figure S4). For such a "UV + Vac." treatment even ZnO annealed only at 80°C shows complete calcium oxidation suppression. This process was chosen as our new treatment method due to the low temperatures and the excellent ZnO quality. Additionally, SnO_2 layers were investigated, showing no significant reaction with calcium under any of the treatment conditions.

As discussed in the introduction, after sufficient time in nitrogen, ZnO typically desorbs water, while oxygen remains chemisorbed [13]. For all our tests, annealing was performed in nitrogen, where the elevated temperature would further help to desorb water. Thus, we expect the reaction of calcium to primarily occur with oxygen released from the ZnO layer, while a detailed investigation of the chemistry in the calcium test is beyond the scope of this study. Nevertheless, a qualitative comparison is possible, showing that increased annealing temperature reduces the amount of calcium degradation, with further improvements upon UV treatment in nitrogen. Most interestingly, the combination of UV light and vacuum removes all signs of oxidation, and the calcium remains fully metallic, while maintaining a low temperature of 80°C. This is especially relevant, as roll-to-roll fabrication of OPV on flexible substrates does not allow for prolonged high temperature annealing, while vacuum or reduced pressure steps are feasible.

While any oxygen released from the ZnO layer will directly react with calcium in the previous tests, in a full solar cell, there will be a complex interaction of the effects by oxygen release combined with changes of conductivity and possibly energy level changes of

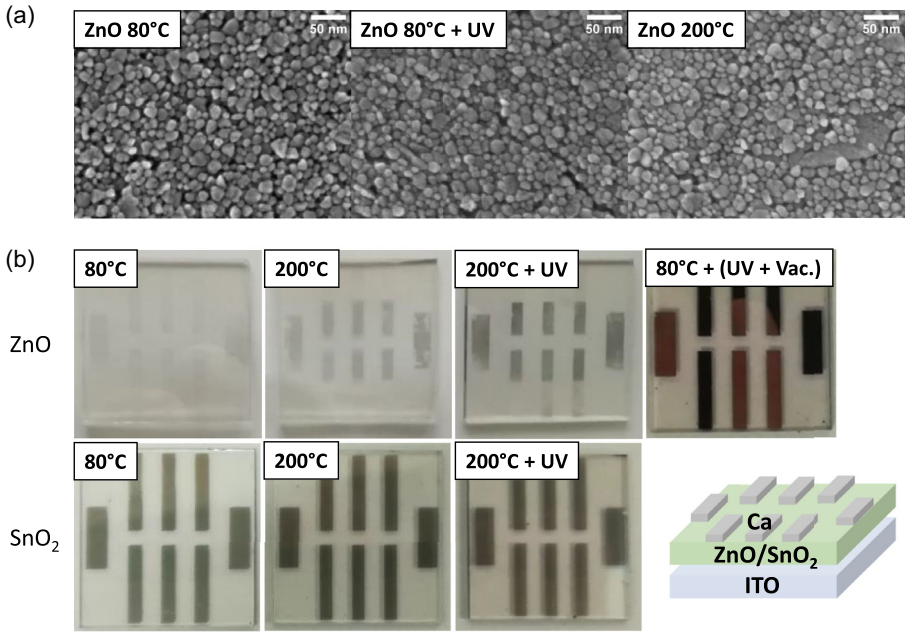

FIGURE 1 | (a) SEM images of ZnO NPs spincoated on ITO with different annealing temperatures as well as with and without UV treatment. (b) Visual tests with a 40 nm calcium layer on top. The calcium becomes transparent on top of ZnO layers, even for annealing at 200°C and UV treatment in nitrogen (200°C + UV), while UV treatment in vacuum shows no visible reaction of the calcium even at just 80°C annealing temperature. SnO_2 layers show no significant reaction of the calcium. SEM = scanning electron microscopy; UV = ultraviolet.

ZnO. In order to probe for changes in conductivity as well as possible changes of energy levels in a controlled way, electron only devices were fabricated, and the current voltage characteristics measured. This returns space charge limited current (SCLC) data, which is further analyzed with drift diffusion models. The devices were produced with the following structure: ITO-ZnO-ActiveLayer-PDINN-Ag. After spincoating, the ZnO layer was annealed at different temperatures (80°C and 200°C), as well as UV exposure in vacuum was tested. Then, the rest of the device stack was deposited. For reference, also a device with SnO_2 was manufactured.

The SCLC devices were measured periodically in the dark and illuminated with a warm white LED (3000K) to slowly light-soak the ZnO layers while being able to observe any changes with the in situ SCLC measurements (see Figure 2). Negative voltages show injection from the PDINN side which serves as a reference and only shows slight changes over time or for different materials. For PM6-Y6 with ZnO annealed at 80°C, a very low current is observed on the ZnO side (positive voltages) suggesting an energetic barrier due to the not yet light-soaked layer. With continuous white light illumination, the current density rises and becomes symmetric to the PDINN side, showing a vanishing extraction barrier. With the ZnO layer annealed at 200°C, the initial current is higher (lower energetic barrier) and approaches the level of PDINN faster during light soaking. Interestingly, the ZnO 80 + UV substrate shows a much higher initial current density but does not notably change upon lightsoaking. For SnO_2 the

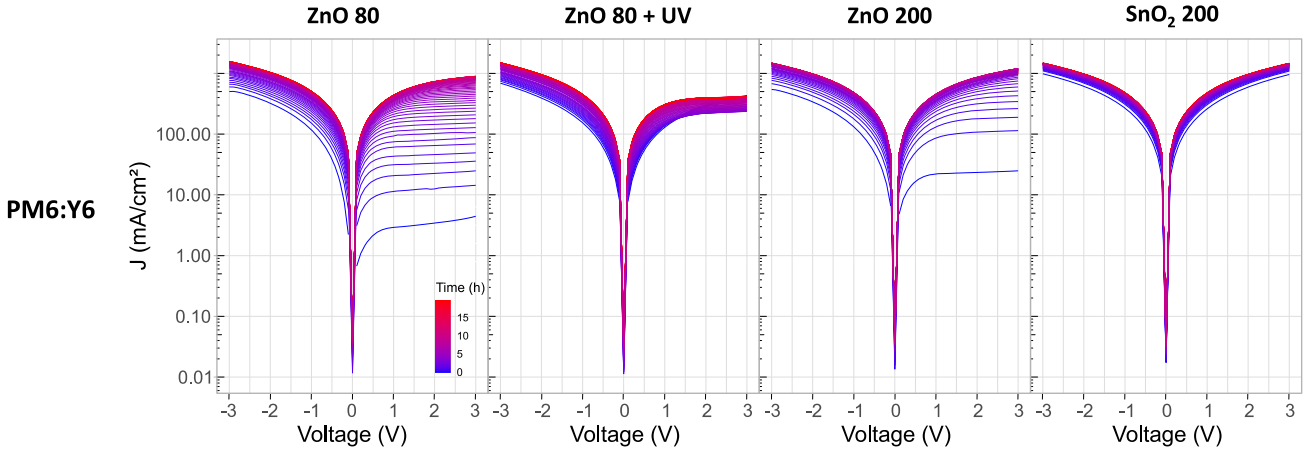

FIGURE 2 | SCLC measurements in the dark over time for a stability test with white light LED illumination. The device structure is ITO-ZnO-PM6-Y6-PDINN-Ag. ZnO was prepared with the following conditions: annealed at 80°C, annealed at 200°C, as well as annealed at 80°C and then exposed to UV light in vacuum for 5 min. Negative voltages show injection from the PDINN side, while positive voltages show injection from the ZnO side. The shown curves are averages of up to 12 cells. LED = light-emitting diode; SCLC = space charge limited current; UV = ultraviolet.

SCLC data is symmetric even without light-soaking and has only marginal changes in the current densities over time.

To make sure that the tested devices were fully light soaked after the white light LED illumination experiment, the devices were additionally light soaked with UV light for 5 min (see Figure S1) where no additional changes are observed.

Drift diffusion simulations were used to fit the SCLC data for PM6-Y6 devices (Table S1 and Figure S1). Very good fits could be obtained by only changing the energetic offset at the ZnO/SnO_2 side, as well as the series resistance, while all other parameters were fixed. The active layer shows no significant difference in the UV–vis absorption spectra (see Figure S6), which is a good indicator that the layer thickness and morphology are very similar. This further justifies to fix all parameters regarding the active layer. An influence of traps was not included in the model, as in the double logarithmic plot of the SCLC data (see Figure S2); no trap-filled-limited (TFL) regime could be detected. The good fit with only two free parameters suggests that a change of ZnO conductivity as well as ZnO energy levels are the main changes between different ZnO treatment conditions. For the fresh ZnO 80 device, the energetic offset at the ZnO interface is the highest at 0.48 eV while annealing at 200°C reduces the offset to 0.43 eV. After light soaking under white light and after the final UV light soaking, the ZnO offset is 0.36 eV for both treatment conditions. This value matches the offset for the UV and vacuum-treated sample already in a fresh state (0.36 eV). For SnO_2, no energetic barriers were observed.

The SCLC tests for PM6-Y6 with ZnO reflect the observations made in the calcium tests: High initial injection barriers for the devices annealed at 80°C and 200°C are consistent with strong reaction of the calcium, while the UV and vacuum-treated sample has a low initial injection barrier and no reaction of the calcium.

As a next step, PM6-Y6 solar cells were tested with the slow light soaking protocol as previously established for SCLC measurements. The slow light soaking with white light LEDs provides enough time for in situ measurements. A self-built automated setup periodically measures EL images with an IR camera and IV curves are also recorded in the same intervals as EL images (see Figure 3).

The EL images show an inhomogeneous image for the fresh ZnO which was annealed at 200°C (see Figure 3d). After 40 h of slow light soaking with the white LED, the image for ZnO becomes homogeneous, while for SnO_2 the EL image is homogeneous from the start. This is consistent with the observations on the SCLC devices where a continuous increase of injection current is observed for the ZnO device annealed at 200°C under white light illumination. We can thus observe both, a reduction of injection barrier in SCLC and a change of the EL image to a more homogeneous area as a direct consequence of ZnO light soaking. Additionally, an increase of PCE is observed during light-soaking for ZnO which is not present in SnO_2.

After slow light soaking for 40 h, an additional UV LED (365 nm) is turned on to fully light-soak the devices and test solar cell stability. Previous experiments showed a reduced stability of devices with SnO_2 under blue light illumination [29], which can also be observed here using UV illumination. The devices with SnO_2 have a faster reduction of PCE under UV illumination as well as a very fast reduction of EL intensity to non-measurable levels. So while SnO_2 mitigates negative effects due to light-soaking, it can be a liability for long-term photo-stability, where additionally potassium ions used as stabilizing ligands for SnO_2 have been shown to negatively impact device stability [20]. Consequently, a tradeoff has to be made when choosing interface layers.

To further investigate the effects of the adsorbed oxygen on the cell dynamics, we did transient photo voltage (TPV) and charge extraction (CE) measurements, shown in Figure S7, for a PM6:Y6 cell before and after lightsoaking. Panel (a) shows the carrier lifetime τ plotted over the bias light intensity (given as OD), showing no difference in recombination behavior, while for (b) where we plotted τ over VOC, we observe a general shift in the voltage,

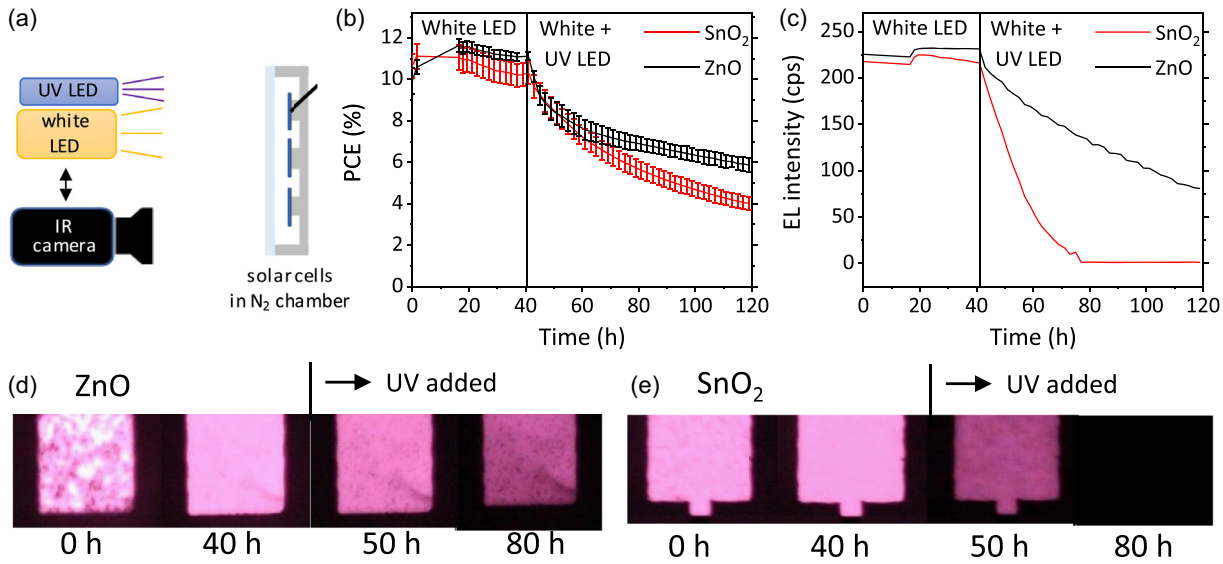

FIGURE 3 | Degradation of PM6-Y6 cells with either ZnO or SnO_2 as the electron transport layer both were annealed at 200°C. (a) The schematic drawing of the setup used for the measurement. (b) PCE over time. (c) The EL intensity over time for the EL images at (d) and (e). (e) The EL images for SnO_2 and (d) the EL images for ZnO at different times. EL = electroluminescence.

indicating a barrier. CE in panel (c) also shows a shift along the voltage axis, while the charge carrier density is mostly unchanged. Figure S7d shows the combination of both measurements as the carrier lifetime τ (extracted from TPV) is plotted over the Q (extracted) from CE. The curves show a slope (recombination order) of 1.877 for initial cell and 1.876 for the lightsoaked cell, further indicating no change of recombination kinetics.

In the following, we will use several different active layer materials with ZnO interlayers in order compare the light-soaking effects observed for PM6-Y6 with other active layer materials. In particular, also P3HT-ehIDBTR and PCE10-ehIDBTR solar cells are investigated. ZnO was annealed at just 80°C in order to obtain good observability of any light-soaking effects. Again, a slow light soaking with white LED illumination was used to allow for in situ IV-measurement during the light soaking process. As the drift-diffusion modeling has identified energetic offsets and series resistance as the two main factors, we will focus on fill factor and series resistance data of the solar cells. Energetic offsets typically present themselves as s-shapes in IV curves which are represented by the fill factor.

Most interestingly, in Figure 4, the fill factor for PM6-Y6 reaches most of its final value after around 5 h, while for the other two material systems, light soaking takes over 40 h to get close to the final state. The same trend is also reflected in the series resistance data. The 5-h time range for PM6-Y6 light soaking is fully consistent with the SCLC data from Figure 5 where the final state is also approached in a similar time range. Notably, PM6-Y6 seems to be the exception with significantly faster kinetics than the other materials tested. In order to gain more insight, another experiment was performed with just a fourth of the light intensity (25 mW cm^{-2} instead of 100 mW cm^{-2}) (see Figure 4f). No light intensity dependence is observed for PM6-Y6 with the low light intensity experiment showing the same kinetics as the high intensity data. To verify, that all "light soaking" processes are complete after 5 h, even in the low light intensity test with just the white LED, a final UV treatment step was performed for the PM6-Y6 sample. No further change is observed with the final UV treatment, suggesting all changes of the ZnO layer were complete already after 5 h independent of light intensity.

Given the fast and light intensity independent "light soaking" for PM6-Y6, it can be speculated that the active layer reacts with residual oxygen from ZnO with only minimal activation necessary. This would be consistent with the results from Du et al. [26] who observed a low starting efficiency for PM6-Y6 devices if the ZnO was insufficiently annealed at low temperatures. A recent review on PM6-Y6 by Shoaee et al. [30] highlights that the highest performance for PM6-Y6 is typically achieved with a PEDOT based bottom interface layer and that the efficiency of ZnO-based devices is lacking behind across the literature. The unique behavior of PM6-Y6 in our slow light soaking test combined with those literature observations suggests that a fast limited reaction of the active layer with oxygen released from ZnO might be the cause for a reduced starting efficiency. This adds to the unique properties of PM6-Y6 which also have been shown to have unique charge generation properties [31].

In order to test, if improved treatment of the ZnO interface layer can improve the starting efficiency, UV illumination of the ZnO layer in vacuum was used, which showed no signs of reaction with calcium in Figure 1. Three different active layer materials were tested (see Figure 5). The IV curves were directly measured with an AM1.5G solar simulator, which provides enough UV light to fully activate ZnO during the measurement. This means no s-shapes or FF losses (see Figure S3) are observed for those measurements. For PM6:Y12 (Y12 instead of Y6 was chosen,

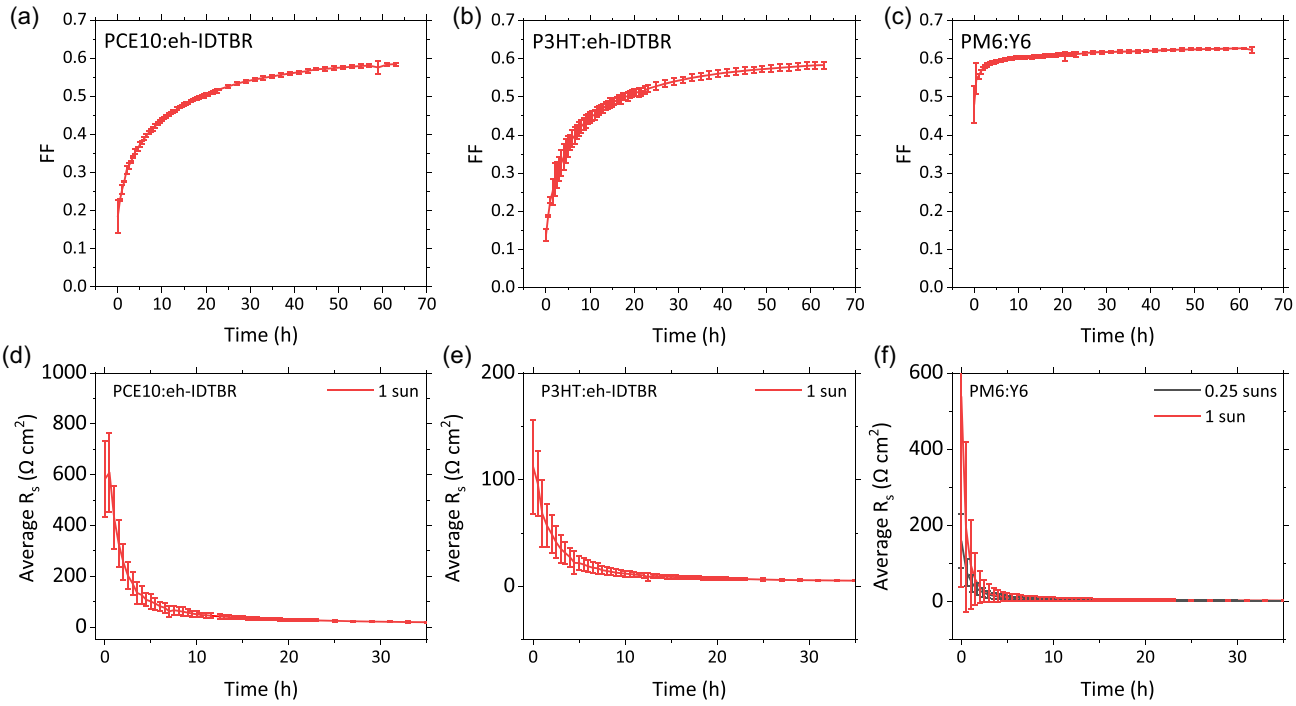

FIGURE 4 | (a–c) Fill factor evolution during slow light soaking for three different active layer materials. PM6-Y6 shows exceptionally fast kinetics. (d–f) Series resistance data for the same experiment measured in the dark.

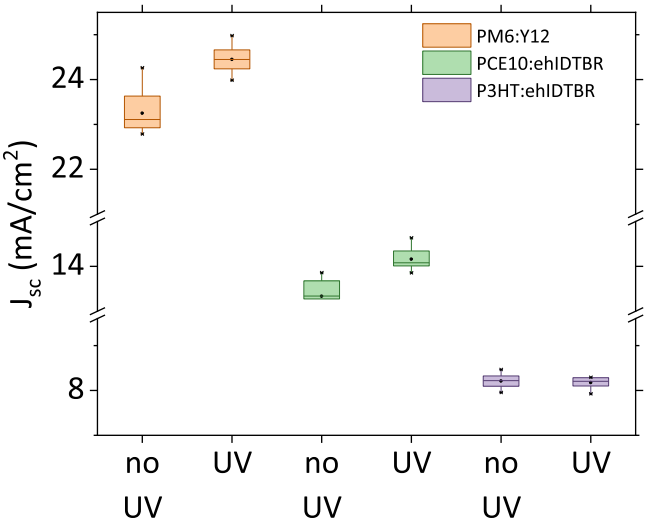

FIGURE 5 | Short circuit current of solar cells with ZnO layers annealed at 80°C as well as ZnO layers additionally treated with UV light in vacuum for three different active layer material systems. Permanent J_{sc} losses for PM6-Y6 occur if the ZnO Substrate is not treated sufficiently. P3HT-ehIDTBR is not sensitive to ZnO treatment. Measured under an AM 1.5G solar simulator. UV = ultraviolet.

to understand if the effect is a general effect on the y-series acceptors) a significantly higher starting J_{sc} is observed with the UV and vacuum treated ZnO interlayer, suggesting that removal of oxygen from the ZnO layer allows to significantly improve J_{sc}. For P3HT-ehIDTBR no change of J_{sc} is observed. The low sensitivity of eh-IDTBR based systems to ZnO treatment is consistent with a low photo-bleaching rate for eh-IDTBR [27].

For PCE10-ehIDTBR, a small reduction of J_{sc} is visible without UV treatment. Since the difference is small, data for a repeated experiment is shown in Figure S5. The short circuit current for the PCE10-ehIDTBR devices without UV treatment of the ZnO layer is lower in several samples and does not improve with a UV light soaking step of the full device. As discussed for PM6-Y6, this suggests permanent (albeit smaller) damage caused by the ZnO layer which was not UV-treated during cell production and happens even before a classical light-soaking step of the finished solar cell. While IDTBR has a high stability against photo-oxidation [27], those losses might be caused by damage to the PCE10 from small amounts of oxygen being released from ZnO. The possibility to avoid permanent J_{sc} losses, especially for PM6-Y6, by UV and low pressure treatment of ZnO is critical for large scale role to roll processing, as well as for tandem solar cells, where ZnO is also used as interface layer [32] and where high temperature annealing is prohibitive. To further show the relevance for this treatment for role to roll processing, we also did an exposure test, shown in Figure S8. Here, we exposed half cells (after deposition of the active layer) and full cells (after evaporation of silver) to ambient air for 10 min, showing the benefits of UV treatment are, even though smaller, still present.

3 | Summary and Conclusion

In a nutshell, three major factors for ZnO-based interlayers were investigated. Energetic barriers at the ZnO interfaces are observed from drift-diffusion fits of SCLC devices and are typically visible in s-shapes of IV curves. Changes in series resistance were observed in SCLC fits, which are expected to represent a change of conductivity in the ZnO layer upon light-soaking. In solar cells, a change of series resistance is visible upon light soaking and could be used to identify a distinctly different light soaking behavior in PM6-Y6 devices. Finally, permanent J_{sc} losses can be linked to different treatment conditions of ZnO and are most likely caused by reactions of the active layer materials with residual oxygen released from ZnO. Those permanent J_{sc} losses can be significant for novel PM6-Y6 based devices and have not yet received sufficient scientific attention, as they occur before the first IV measurement and are absent for established material systems like P3HT-ehIDTBR.

Acknowledgements

The authors gratefully acknowledge financial support from the Helmholtz Association in the framework of the innovation platform "Solar TAP." This project has received funding from the European Union's Horizon 2020 research and innovation program under grant agreement No 952911 (BOOSTER) and 101137889 (PH2OTOGEN). The authors want to thank the Deutsche Forschungsgemeinschaft (DFG) for financial support in the scope of the Research Unit FOR 5387 POPULAR, project no. 461909888. C.J.B. and J.H. gratefully acknowledge grants "ELF-PV"- Design and development of solution-processed functional materials for the next generations of PV technologies (no. 44-6521a/20/4). C.J.B. gratefully acknowledges financial support through the "Aufbruch Bayern" initiative of the state of Bavaria (EnCN and "Solar Factory of the Future") and the Bavarian Initiative "Solar Technologies go Hybrid" (SolTech).

Open Access funding enabled and organized by Projekt DEAL.

Conflicts of Interest

The authors declare no conflicts of interest.

Data Availability Statement

The data that support the findings of this study are available from the corresponding author upon reasonable request.

References

1. L. Zhu, M. Zhang, J. Xu, et al., "Single-Junction Organic Solar Cells with over 19% Efficiency Enabled by a Refined Double-Fibril Network Morphology," *Nature Materials* 21 (2022): 656–663.

2. A. Armin, W. Li, O. J. Sandberg, et al., "A History and Perspective of Non-Fullerene Electron Acceptors for Organic Solar Cells," *Advanced Energy Materials* 11 (2021): 2003570.

3. L. J. Koster, O. Stenzel, S. D. Oosterhout, M. M. Wienk, V. Schmidt, and R. A. Janssen, "Morphology and Efficiency: The Case of Polymer/ZnO Solar Cells," *Advanced Energy Materials* 3, no. 5 (2013): 615–621.

4. Y. Liu, Y. Li, and H. Zeng, "ZnO-Based Transparent Conductive Thin Films: Doping, Performance, and Processing, " *Journal of Nanomaterials* 2013 (2013): 196521.

5. S. K. Hau, H.-L. Yip, N. S. Baek, J. Zou, K. O'Malley, and A. K.-Y. Jen, "Air-Stable Inverted Flexible Polymer Solar Cells Using Zinc Oxide Nanoparticles as an Electron Selective Layer," *Applied Physics Letters* 92 (2008): 253301.

6. M. A. Ibrahem, H.-Y. Wei, M.-H. Tsai, K.-C. Ho, J.-J. Shyue, and C. W. Chu, "Solution-Processed Zinc Oxide Nanoparticles as Interlayer

Materials for Inverted Organic Solar Cells," *Solar Energy Materials and Solar Cells* 108 (2013): 156–163.

7. H.-Y. Park, D. Lim, K.-D. Kim, and S.-Y. Jang, "Performance Optimization of Low-Temperature-Annealed Solution-Processable ZnO Buffer Layers for Inverted Polymer Solar Cells," *Journal of Materials Chemistry A* 1, no. 21 (2013): 6327–6334.

8. F. Mohtaram, S. Borhani, M. Ahmadpour, et al., "*Electrospun ZnO Nanofiber Interlayers for Enhanced Performance of Organic Photovoltaic Devices*," *Solar Energy* 197 (2020): 311-316.

9. E. Mollow, "*Proceedings of the Conference on Photoconductivity*" John Wiley and Sons, Inc, New York (1956).

10. R. J. Collins and D. G. Thomas, "Photoconduction and Surface Effects with Zinc Oxide Crystals," *The Physical Review* 112, no. 2 (1958): 388–395.

11. G. Gonçalves, A. Pimentel, E. Fortunato, et al., "UV and Ozone Influence on the Conductivity of ZnO Thin Films," *Journal of Non-Crystalline Solids* 352 (2006): 1444–1447.

12. R. Martins, E. Fortunato, P. Nunes, et al., "Zinc Oxide as an Ozone Sensor," *Journal of Applied Physics* 96 (2004): 1398–1408.

13. A. J. Morfa, B. I. MacDonald, J. Subbiah, and J. J. Jasieniak, "Understanding the Chemical Origin of Improved Thin-Film Device Performance from Photodoped ZnO Nanoparticles," *Solar Energy Materials and Solar Cells* 124 (2014): 211–216.

14. J. Bao, I. Shalish, Z. Su, et al., "Photoinduced Oxygen Release and Persistent Photoconductivity in ZnO Nanowires," *Nanoscale Research Letters* 6 (2011): 1–7.

15. Z. Jiang, S. Soltanian, B. Gholamkhass, A. Aljaafari, and P. Servati, "Light-Soaking Free Organic Photovoltaic Devices with Sol-Gel Deposited ZnO and AZO Electron Transport Layers," *RSC Advances* 8, no. 64 (2018): 36542–36548.

16. S. Marouf, A. Beniaiche, K. Kardarian, et al., "Low-Temperature Spray-Coating of High-Performing ZnO: Al Films for Transparent Electronics," *Journal of Analytical and Applied Pyrolysis* 127 (2017): 299–308.

17. T. Kuwabara, K. Yano, T. Yamaguchi, et al., "Mechanistic Investigation into the Light Soaking Effect Observed in Inverted Polymer Solar Cells Containing Chemical Bath Deposited Titanium Oxide," *The Journal of Physical Chemistry C* 119 (2015): 5274–5280.

18. S. Trost, K. Zilberberg, A. Behrendt, et al., "Overcoming the, Light-Soaking, Issue in Inverted Organic Solar Cells by the Use of Al: ZnO Electron Extraction Layers," *Advanced Energy Materials* 3 (2013): 1437–1444.

19. M. Prosa, M. Tessarolo, M. Bolognesi, et al., "Enhanced Ultraviolet Stability of Air-Processed Polymer Solar Cells by Al Doping of the ZnO Interlayer," *ACS Applied Materials & Interfaces* 8 (2016): 1635–1643.

20. D. Garcia Romero, L. Di Mario, F. Yan, et al., "Understanding the Surface Chemistry of SnO2 Nanoparticles for High Performance and Stable Organic Solar Cells, *" Advanced Functional Materials* 34, no. 6 (2024): 2307958.

21. C. Liu, R. Félix, K. Forberich, et al., "Utilizing the Unique Charge Extraction Properties of Antimony Tin Oxide Nanoparticles for Efficient and Stable Organic Photovoltaics," *Nano Energy* 89 (2021): 106373.

22. M. Mirsafaei, P. B. Jensen, M. Ahmadpour, et al., "Sputter-Deposited Titanium Oxide Layers as Efficient Electron Selective Contacts in Organic Photovoltaic Devices," *ACS Applied Energy Materials* 3, no. 1 (2020): 253–259.

23. M. Ahmadpour, M. Ahmad, M. Prete, et al., "Tuning Surface Defect States in Sputtered Titanium Oxide Electron Transport Layers for Enhanced Stability of Organic Photovoltaics" *ACS Applied Materials & Interfaces* 16, no. 13 (2024): 16580–16588.

24. D. Amelot, M. Ahmadpour, Q. Ros, et al., "Deciphering Electron Interplay at the Fullerene/Sputtered TiOxInterface: A Barrier-Free Electron Extraction for Organic Solar Cells *ACS Applied Materials & Interfaces* 13, no. 16 (2021): 19460–19466.

25. M. R. Lilliedal, A. J. Medford, M. V. Madsen, K. Norrman, and F. C. Krebs, "The Effect of Post-Processing Treatments on Inflection Points in Current-Voltage Curves of Roll-to-Roll Processed Polymer Photovoltaics," *Solar Energy Materials and Solar Cells* 94 (2010): 2018–2031.

26. X. Du, L. Lüer, T. Heumueller, et al., "Elucidating the Full Potential of OPV Materials Utilizing a High-Throughput Robot-Based Platform and Machine Learning," *Joule* 5 (2021): 495–506.

27. J. Guo, Y. Wu, R. Sun, et al., "Suppressing Photo-Oxidation of Non-Fullerene Acceptors and Their Blends in Organic Solar Cells by Exploring Material Design and Employing Friendly Stabilizers," *Journal of Materials Chemistry A* 7, no. 43 (2019): 25088–25101.

28. M. Guenther, S. Lotfi, S. S. Rivas, et al., "The Neglected Influence of Zinc Oxide Light-Soaking on Stability Measurements of Inverted Organic Solar Cells," *Advanced Functional Materials* 33 (2023): 2209768.

29. P. Weitz, V. M. Le Corre, X. Du, et al., "Revealing Photodegradation Pathways of Organic Solar Cells by Spectrally Resolved Accelerated Lifetime Analysis," *Advanced Energy Materials* 13, no. 2 (2023): 2202564.

30. S. Shoaee, H. M. Luong, J. Song, Y. Zou, T. Q. Nguyen, and D. Neher, "What We Have Learnt from PM6: Y6," *Advanced Materials* 36, no. 20 (2024): 2302005.

31. E. Sağlamkaya, A. Musiienko, M. S. Shadabroo, et al., "What Is Special about Y6; the Working Mechanism of Neat Y6 Organic Solar Cells," *Materials Horizons* 10, no. 5 (2023): 1825–1834.

32. D. Di Carlo Rasi and R. A. Janssen, "Advances in Solution-Processed Multijunction Organic Solar Cells," *Advanced Materials* 31, no. 10 (2019): 1806499.

Supporting Information

Additional supporting information can be found online in the Supporting Information section.